Title

Eukaryotic algal phytochromes span the visible spectrum

Journal

Proceedings of the National Academy of Sciences of the United States of America, 111(10)

ISSN

0027-8424

Authors

Rockwell, Nathan C
Duanmu, Deqiang
Martin, Shelley S
et al.

Publication Date

2014-03-11

DOI

10.1073/pnas.1401871111

Peer reviewed

Eukaryotic algal phytochromes span the visible spectrum

Nathan C. Rockwell[a], Deqiang Duanmu[a], Shelley S. Martin[a], Charles Bachy[b], Dana C. Price[c], Debashish Bhattacharya[c], Alexandra Z. Worden[b,d], and J. Clark Lagarias[a,1]

[a]Department of Molecular and Cellular Biology, University of California, Davis, CA 95616; [b]Monterey Bay Aquarium Research Institute, Moss Landing, CA 95039; [c]Department of Ecology, Evolution, and Natural Resources, Institute of Marine and Coastal Sciences, Rutgers University, New Brunswick, NJ 08903; and [d]Integrated Microbial Biodiversity Program, Canadian Institute for Advanced Research, Toronto, ON, Canada M5G 1Z8

Contributed by J. Clark Lagarias, January 29, 2014 (sent for review December 9, 2013)

Plant phytochromes are photoswitchable red/far-red photoreceptors that allow competition with neighboring plants for photosynthetically active red light. In aquatic environments, red and far-red light are rapidly attenuated with depth; therefore, photosynthetic species must use shorter wavelengths of light. Nevertheless, phytochrome-related proteins are found in recently sequenced genomes of many eukaryotic algae from aquatic environments. We examined the photosensory properties of seven phytochromes from diverse algae: four prasinophyte (green algal) species, the heterokont (brown algal) *Ectocarpus siliculosus*, and two glaucophyte species. We demonstrate that algal phytochromes are not limited to red and far-red responses. Instead, different algal phytochromes can sense orange, green, and even blue light. Characterization of these previously undescribed photosensors using CD spectroscopy supports a structurally heterogeneous chromophore in the far-red–absorbing photostate. Our study thus demonstrates that extensive spectral tuning of phytochromes has evolved in phylogenetically distinct lineages of aquatic photosynthetic eukaryotes.

biliprotein | photoswitch | photochemistry | bilin | tetrapyrrole

Modern human societies rely on agriculture and related practices such as aquaculture to provide consistent, efficient food production. These processes ultimately rely on photosynthetic organisms to produce foodstuffs or fodder. Terrestrial crop plants are grown at very high density under modern agricultural practices, causing competition between individual plants for light. Land plants detect such competition through the photoreceptor phytochrome, which uses the ratio of red to far-red* light to sense the ambient light environment (1, 2). In shaded, far-red–enriched environments, plants trigger the shade avoidance response. Effects of this response include diversion of biomass from leaf to stem, reduced root systems, and reduced crop yield. Phytochrome acts as a master regulator both of shade avoidance and of light-dependent development or photomorphogenesis (1–6).

Plant phytochromes are conserved multidomain proteins using linear tetrapyrrole (bilin) chromophores (1). Phytochromes are also found in streptophyte algae, cyanobacteria, other bacteria, fungi, and diatoms (7–9) All phytochromes use a conserved, knotted N-terminal photosensory core module (PCM) (Fig. S1) (10–12) in which a bilin chromophore is covalently linked to a conserved Cys residue (1). Different bilins can serve as chromophore precursor (Fig. S1), with distinct Cys residues providing the covalent attachment sites for phytobilins and for biliverdin IXα (BV) (CysC and CysA, respectively; Fig. S2). Light absorption by phytochromes triggers photoisomerization of the bilin 15,16-double bond between *15Z* and *15E* configurations (13–16). In plant phytochromes, the dark-stable form is the red-absorbing *15Z* P_r photostate (1, 9). Photoconversion yields a metastable far-red–absorbing *15E* P_{fr} photoproduct. P_r can be rapidly regenerated photochemically by far-red light; therefore, photobiological phenomena regulated by phytochrome are typically modulated by the relative amounts of red and far-red light.

Although essential for normal plant growth and development (17, 18), phytochrome would seem less useful for aquatic organisms because red and far-red light do not penetrate water to depths greater than a few meters (19). Indeed, phytochrome is absent in the rhodophyte (red alga) *Chondrus crispus*, found from intertidal regions to ∼20-m depth (20, 21). Similarly, the green alga *Chlamydomonas reinhardtii* lacks phytochrome despite retaining the ability to synthesize the bilin chromophore phycocyanobilin (PCB) (22). However, recent genomic studies reveal the presence of phytochrome genes in a broad range of eukaryotic algae spanning several lineages (Fig. 1). These taxonomically diverse algae include the tiny prasinophyte *Micromonas pusilla* (≤2 μm in size), the freshwater glaucophyte *Cyanophora paradoxa*, and the complex, multicellular *Ectocarpus siliculosus* (23–25). These widespread phytochromes in distantly related algae lead to the question of spectral sensitivity: do these proteins retain red/far-red photocycles for specialized function when the algal cell is near the surface, or do they exhibit distinct spectral responses reflecting the individual algal environments?

To date, photochemical properties have only been reported for algal phytochromes from charophytes (26–28), organisms associated with shallow freshwater ecosystems (29). These proteins exhibit red/far-red photocycles similar to those of land plant phytochromes, which are the closest extant relatives of charophytes

Significance

Photosynthetic organisms exploit photosensory proteins to respond to changing light conditions. In land plants, phytochromes use the ratio of red to far-red light to detect shading by neighboring plants, leading to changes in growth and development. Light conditions can be more variable for algae because of the wavelength-dependent attenuation of light by water and because of ocean mixing. We studied phytochromes from taxonomically diverse eukaryotic algae from groups considered important for coastal ecosystems and the global carbon cycle. These proteins detect light throughout the visible spectrum (blue, green, orange, red, and far-red). Extensive spectral tuning has evolved within these algae, presumably reflecting aquatic light environments. These studies should ultimately facilitate engineering of crop plant species for diverse light environments.

Author contributions: N.C.R., D.D., and J.C.L. designed research; N.C.R., D.D., S.S.M., C.B., and A.Z.W. performed research; D.D., C.B., D.C.P., D.B., A.Z.W., and J.C.L. contributed new reagents/analytic tools; N.C.R., D.D., C.B., D.C.P., D.B., A.Z.W., and J.C.L. analyzed data; and N.C.R. and J.C.L. wrote the paper.

The authors declare no conflict of interest.

Data deposition: The sequences reported in this paper have been deposited in the GenBank database [accession nos. KF894948 (TastPHY1), KF894950 (NpyrPHY1), KF894946 (DtenPHY1), KF894949 (PcolPHY1), KF894955 (EsilPHL1), KF894951 (CparGPS1), and KF894953 (GwitGPS1)].

[1]To whom correspondence should be addressed. E-mail: jclagarias@ucdavis.edu.

This article contains supporting information online at www.pnas.org/lookup/suppl/doi:10.1073/pnas.1401871111/-/DCSupplemental.

*We are using the following definitions for color regions: near-UV, 300–395 nm; violet, 395–410 nm; blue, 410–480 nm; teal, 480–510 nm; green, 510–570 nm; yellow, 570–590 nm; orange, 590–615 nm; red, 615–675 nm; far-red, 675–740 nm; and near-infrared, 740–1,000 nm.

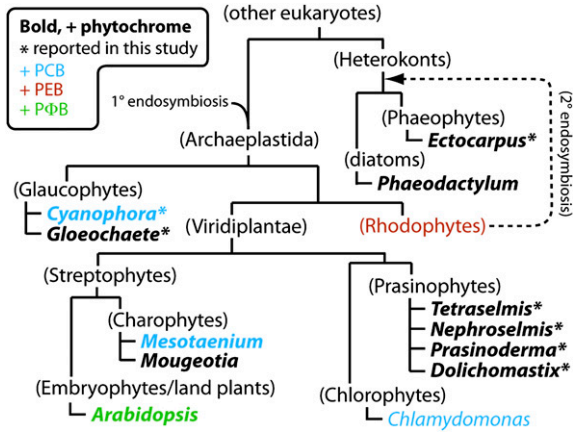

Fig. 1. Phytochrome distribution in photosynthetic eukaryotes. A simplified evolutionary scheme for evolutionary relationships among eukaryotes is shown. Source organisms are indicated by genera; larger groupings are in parentheses. The presence of phytochromes (bold) is indicated. Organisms with known bilin composition are color-coded.

(Fig. 1). The present study was therefore undertaken to assess the photosensory behavior of phytochromes from a more diverse range of eukaryotic algae: four prasinophyte phytochromes; one heterokont phytochrome, EsilPHL1 from the phaeophyte (multicellular brown alga) *E. siliculosus*; and two glaucophyte phytochromes.[†] Several of these phytochrome genes were detected as part of an ongoing transcriptomic study of algal evolution and are not yet complete. Nevertheless, existing gene models allow us to examine the photosensory properties of the truncated PCM region (Fig. S1) using heterologous expression in *Escherichia coli* cells engineered to coproduce various bilin chromophores (30–33). These algal phytochromes exhibit diverse photocycles ranging from blue to far-red, revealing algal phytochromes as an unexpectedly diverse group of photoreceptors. Our studies herald future insights into algal photobiology and demonstrate the value of moving beyond model systems to assess diversity within a given protein family across the eukaryotic tree of life.

Results

For phytochromes analyzed to date, the PCM module alone is sufficient to confer spectral properties indistinguishable from those of the full-length protein (1, 9, 12, 32). We therefore used synthetic genes to express PCM truncations recombinantly (Figs. S1 and S3). Bilin biosynthetic enzymes are not normally present in *E. coli*; therefore, this approach requires an explicit choice of bilin precursor. We therefore had to predict physiologically "correct" bilins for the algal phytochromes examined in this study. PCB is the logical chromophore precursor for prasinophyte phytochromes (Fig. 1), because both charophyte and chlorophyte algae have been shown to produce PCB (22, 27). The presence of PCB-containing subunits in glaucophyte phycobiliprotein light-harvesting complexes (34) implicates PCB as the physiologically relevant bilin for glaucophyte phytochrome sensors (GPSs) as well. We therefore characterized prasinophyte and glaucophyte phytochromes after coexpression with PCB biosynthetic machinery.

The chromophores of phytochromes from photosynthetic heterokonts such as diatoms and the phaeophyte *Ectocarpus* are less straightforward to predict. It is possible that these proteins are able to sense other signals or to signal without chromophore (35). Heterokont algae lack phycobiliproteins, but their genomes retain ferredoxin-dependent bilin reductases (FDBRs) required to synthesize phytobilins from BV (24, 36). The *Ectocarpus* phytochrome EsilPHL1 contains both the conserved Cys found in phytobilin-binding plant and cyanobacterial phytochromes and the Cys residue known to bind BV in bacteriophytochromes (BphPs) and fungal (Fph) phytochromes (Fig. S2). Heterokont FDBRs have not yet been experimentally characterized, but heterokont plastids are derived from rhodophytes (37) that were presumably able to synthesize phycoerythrobilin (PEB) ancestrally (Fig. 1). PEB is synthesized in two steps, with initial reduction of the bilin 15,16-double bond followed by reduction of the A-ring vinyl side chain (38). The latter reaction is equivalent to that performed by the FDBR HY2 in converting BV into phytochromobilin (PΦB) in land plants (38). We therefore examined EsilPHL1 with three possible chromophore precursors: BV itself and the phytobilins PEB and PΦB.

Prasinophyte Phytochromes Extend Light Sensing into the Orange Window. All four prasinophyte phytochromes were expressed and purified as photoactive PCB adducts (Fig. S3 and Table S1). TastPHY1 from *Tetraselmis astigmatica* exhibited a red/far-red photocycle (Fig. 2*A*) with peak wavelengths at 648 nm (P_r) and 734 nm (P_{fr}). This photocycle was similar to those of cyanobacterial and charophyte phytochromes using PCB (26, 28, 39). The other three proteins instead exhibited unexpected photocycles (Fig. 2 *B–D*) in which the *15Z* dark state was significantly blue shifted into the orange or yellow region of the spectrum (584–614 nm; Table S1). The *15E* photoproduct state in these proteins was also variable, with a peak ranging from 690 to 726 nm (Table S1). These results demonstrate that prasinophyte phytochromes exhibit the expected far-red–absorbing photoproducts, but dark-state absorption for such proteins is often blue-shifted.

Heterokont Phytochrome Extends Light Sensing into the Green Window. Expression of EsilPHL1 with coproduction of BV or PEB resulted in little to no purified EsilPHL1 holoprotein (Fig. 3*A* and Fig. S3). Protein-bound pigment fluorescence at lower apparent molecular weight could be detected by zinc blotting in the PEB preparation (Fig. S3). This likely reflects the presence of small amounts of porphyrin rather than bilin (Fig. 3*A*, double dagger), as has been seen in other heterologously expressed phytochromes (31, 40). In contrast to these results, coproduction of EsilPHL1 with PΦB yielded a photoactive holoprotein (Fig. 3*A* and Fig. S3). EsilPHL1 exhibited a previously undescribed far-

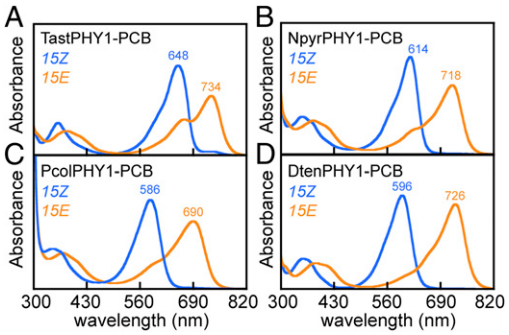

Fig. 2. Light sensing by prasinophyte phytochromes. (*A*) Phytochrome TastPHY1 from *T. astigmatica* exhibits a red/far-red photocycle. Peak wavelengths are indicated for the *15Z* red-absorbing dark state (blue) and *15E* far-red–absorbing photoproduct (orange), with bilin configuration assigned by acid denaturation (42). (*B*) NpyrPHY1 from *N. pyriformis* exhibits an orange/far-red photocycle. (*C*) PcolPHY1 from *P. coloniale* exhibits a yellow/far-red photocycle. (*D*) DtenPHY1 from *D. tenuilepis* exhibits an orange/far-red photocycle.

[†]Phytochromes from the following algae were characterized: the prasinophytes *Tetraselmis astigmatica* CCMP880 (TastPHY1), *Nephroselmis pyriformis* CCMP717 (NpyrPHY1), *Prasinoderma coloniale* CCMP1413 (PcolPHY1), *Dolichomastix tenuilepis* CCMP3274 (DtenPHY1); the phaeophyte *Ectocarpus siliculosus* (EsilPHL1; GenBank locus tag Esi_0437_0011); and the glaucophytes *Cyanophora paradoxa* CCMP329 (CparGPS1) and *Gloeochaete wittrockiana* SAG 46.84 (GwitGPS1).

red/green photocycle, with dark-state absorption at 688 nm and photoproduct absorption at 556 nm (Fig. 3*A* and Table S1). Photoproduct absorption was similar to that seen with the PΦB adduct of the distantly related cyanobacteriochrome (CBCR) photosensor NpR6012g4 from *Nostoc punctiforme* (Fig. 3*B*), but the dark state was red-shifted. We propose that CysC in EsilPHL1 (Fig. S2), a residue conserved in plant phytochromes using PΦB, is responsible for chromophore attachment.

The mechanistic basis for this far-red/green photocycle has not yet been elucidated. One possibility is that the covalent linkage to the bilin is only stable in the photoproduct state, such that the dark state has a longer conjugated system. The presence of an apparent side population (Fig. 3*A*, asterisk) confounds testing this model via the zinc blot assay (41), because this assay does not discriminate between such subpopulations. Bilin biosynthesis in *Ectocarpus* has not yet been addressed, but our results demonstrate that EsilPHL1 can use phytobilin chromophores to function as a photosensor.

Glaucophyte Phytochrome Sensors Extend Light Sensing into the Blue Window. The domain architectures of glaucophyte GPS proteins are distinct from the stereotyped architectures of plant and prasinophyte phytochromes (Fig. S1). GPS phytochromes are also diverse spectrally. CparGPS1 from *C. paradoxa* exhibited an unusual blue/far-red photocycle (Fig. 3*C* and Table S1). The two CparGPS1 photostates are similar to the violet and red photostates of the trichromatic cyanobacterial phytochrome NpF1183 from *N. punctiforme* (42), but both photostates are red-shifted in CparGPS1 (Fig. 3*D*). NpF1183 has a two-Cys photocycle, with a second covalent linkage to the chromophore forming in the *15Z* dark state to produce the large blue shift (42). The second Cys in NpF1183 is immediately adjacent to the conserved Cys attached to the bilin A-ring, and such a second Cys is also present in CparGPS1 (CysD in Fig. S2).

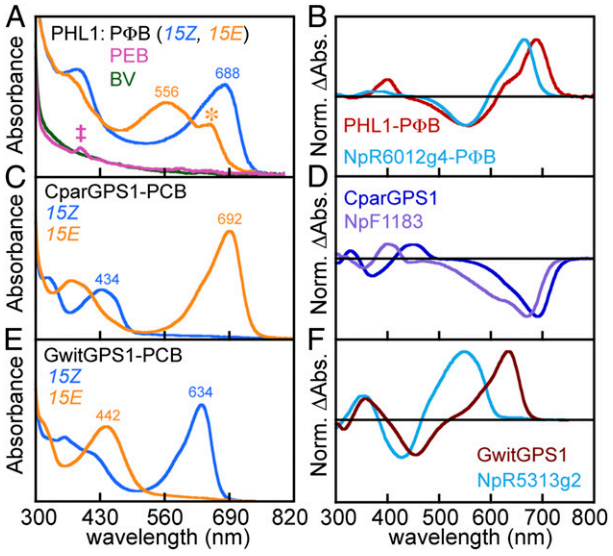

Fig. 3. Light sensing by heterokont and glaucophyte phytochromes. (*A*) PHL1 from the heterokont *E. siliculosus* exhibits a far-red/green photocycle with phytochromobilin (PΦB), colored as in Fig. 2. Coexpression with BV (green) or PEB (pink) does not yield holoprotein. Asterisk, PΦB side population; double dagger, possible porphyrin contaminant. (*B*) Normalized difference spectra are shown for *E. siliculosus* PHL1 (red) and for the PΦB adduct of the red/green CBCR NpR6012g4 from the cyanobacterium *N. punctiforme* (teal) (47). (*C*) CparGPS1 from the glaucophyte *C. paradoxa* exhibits a blue/far-red photocycle. (*D*) Normalized difference spectra are shown for the two-Cys phytochromes NpF1183 from *N. punctiforme* (violet) (42) and CparGPS1 (blue). (*E*) GwitGPS1 from the glaucophyte *G. wittrockiana* exhibits a red/blue photocycle. (*F*) Normalized difference spectra are shown for the *N. punctiforme* CBCR NpR5313g2 (teal) (33) and GwitGPS1 (dark red).

GwitGPS1 from *Gloeochaete wittrockiana* exhibited a reversed photocycle, in which a red-absorbing *15Z* dark state interconverted with a blue-absorbing *15E* photoproduct (Fig. 3*E* and Table S1). This photocycle has similarities to the green/blue photocycles of two-Cys CBCRs such as NpR5313g2 from *N. punctiforme* (33), in which the second linkage forms in the photoproduct state. However, both GwitGPS1 photostates are significantly red-shifted relative to NpR5313g2 (Fig. 3*F*); indeed, the dark-state P_r spectrum of GwitGPS1 is similar to that of the prasinophyte photoreceptor TastPHY1 (Figs. 2*A* and 3*E*). We propose that GwitGPS1 undergoes a two-Cys photocycle with a doubly linked *15E* photoproduct similar to that of NpR5313g2, albeit in the absence of the currently recognized second Cys residues (42, 43). These studies thus reveal striking, unexpected photosensory diversity in GPS proteins.

P_{fr} Heterogeneity in Algal Phytochromes. Despite considerable research interest, the structural basis for perception of far-red light in the P_{fr} state is not yet known (16). We therefore exploited the diverse photocycles of algal phytochromes to further understanding of the P_{fr} photostate using circular dichroism (CD) spectroscopy. The two bilin transitions in the range from 250 to 900 nm give opposite CD signs and can provide information about the 3D orientation of the bilin conjugated π system (44). In plant and cyanobacterial phytochromes, the CD of the long-wavelength transition (red- or far-red–absorbing, also known as *Q* band) inverts upon photoconversion, from negative to positive (32, 45, 46). The short-wavelength Soret transition also changes in these cases. The simple positive Soret signal seen for P_r states is replaced by a complex pattern having an apparent positive band at ∼430 nm, a negative band at ∼380 nm, and another positive band at ∼340 nm (46).

The red/far-red prasinophyte phytochrome TastPHY1 followed this pattern, exhibiting CD spectra very similar to those of cyanobacterial and plant phytochromes (Fig. 4*A*). In the P_{fr} state, we observed positive far-red CD and complex Soret features that were similar to those of the model cyanobacterial phytochrome Cph1 (32, 46). In surprising contrast, the orange/far-red NpyrPHY1 exhibited negative far-red CD but similar Soret features (Fig. 4*B*). Superposition of the TastPHY1 and NpyrPHY1 P_{fr} CD spectra confirmed both the similarity between the two Soret regions and the presence of residual signals from the *15Z* photostate (Fig. 5*A*), complicating analysis of the complex Soret signatures of P_{fr} states.

Because of the residual *15Z* CD signals in prasinophyte phytochromes, we examined the blue/far-red phytochrome CparGPS1. CparGPS1 exhibited no residual *15Z* signals at long wavelength (Fig. 4*C*), but the CparGPS1 P_{fr} CD spectrum still contained complex Soret features at 432, 368, and 334 nm that were consistent with those seen in TastPHY1 and NpyrPHY1 (Fig. 4). Therefore, complex P_{fr} Soret signatures of this type do not arise because of overlapping signals from a residual *15Z* population. Such features are also not intrinsic properties of *15E* bilin configurations, because they are not seen in the CD spectra of *15E* photostates in the distantly related CBCRs (42, 47, 48). These features also cannot be explained as intrinsic properties of far-red–absorbing bilins, because they are absent in the P_{fr} CD spectrum of the bacteriophytochrome DrBphP (32). We therefore conclude that conserved Soret features at ∼350 nm (+), 380 nm (−), and 430 nm (+) arise in the P_{fr} states of certain phytochromes but do not correlate with the apparent sign of the far-red band. These P_{fr} Soret bands thus conflict both with the expected pattern of sign alteration (44) and with the experimental behavior of other biliproteins, including the *15Z* photostates of TastPHY1 and NpyrPHY1 themselves.

To reconcile the discrepancy between Soret and far-red regions of P_{fr} CD spectra, we interpret the Soret region as arising from two subpopulations with opposing signs. In this model, the observed CD of the far-red band must also be a net signal determined by the relative enrichment and relative rotational strengths of two opposed subpopulations. Consistent with this hypothesis,

PLANT BIOLOGY

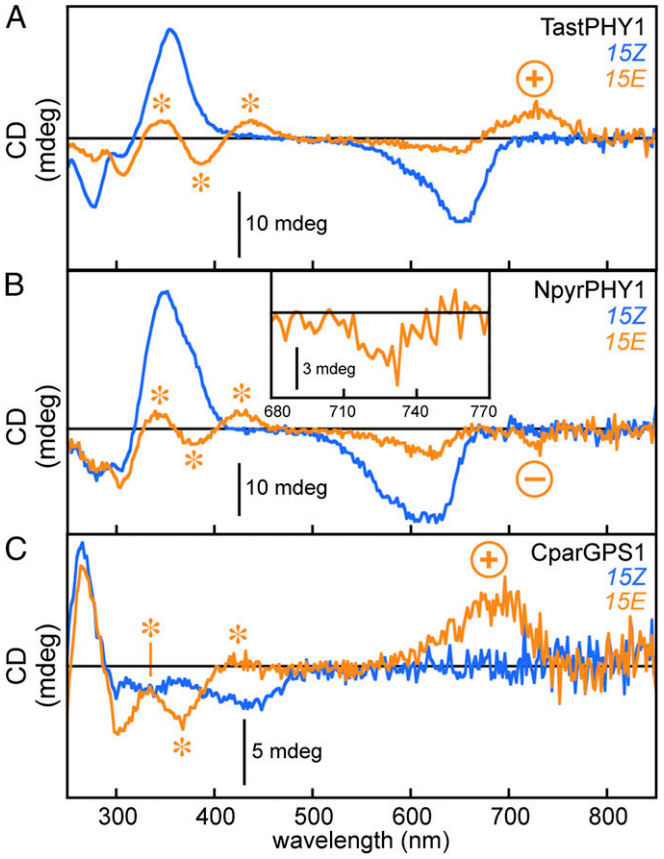

Fig. 4. Variable CD of algal phytochrome P_{fr} photoproducts. (*A*) CD spectra are shown for TastPHY1 in the *15Z* and *15E* photostates, colored as in Fig. 2. (*B*) CD spectra are shown for NpyrPHY1 in the same color scheme; the *Inset* shows the far-red region for the *15E* photostate in detail. For the main graph, the *y* axis is not symmetric to allow greater detail in the far-red region. (*C*) CD spectra are shown for CparGPS1 in the same color scheme. For each *15E* photostate, the sign of the far-red band is shown and asterisks indicate features of the Soret transition. Scale bars and zero CD are indicated.

the Soret regions of the P_{fr} CD spectra of TastPHY1, NpyrPHY1, and CparGPS1 were adequately fit by linear combinations of Gaussian functions of opposed sign (Fig. 5 *B* and *C* and Table S2; procedure described in *SI Materials and Methods*). In CparGPS1, the absence of *15Z* signals at longer wavelengths provided "clean" P_{fr} CD and absorption far-red bands that could also be fit to linear combinations of Gaussians with no complications arising because of residual *15Z* species. In the far-red band, fitted line widths and peak wavelengths for CparGPS1 were similar regardless of the underlying spectroscopy (Fig. 5 *D* and *E* and Table S2). Complete CD spectra for two subpopulations of opposing signs were then calculated, enabling reconstruction of a combined P_{fr} spectrum in good agreement with the experimentally observed spectrum in the bilin region (Fig. 5*F*). We made no attempt to simulate the region below 330 nm, because this region of the CD spectrum can include signals from aromatic amino acids and even from $n\rightarrow\pi^*$ carbonyl transitions (49). This analysis supports the interpretation that P_{fr} states of plant, algal, and cyanobacterial phytochromes are all heterogeneous mixtures of at least two subpopulations.

Discussion

Land plant phytochromes are classically associated with red/far-red photobiological responses. Our studies reveal that phytochromes from eukaryotic algae are also associated with responses to blue, green, and orange light (Fig. 6). Indeed, much of the spectral diversity of the prokaryotic CBCRs (8, 42, 50) is also found in eukaryotic algal phytochromes. Thus, the phytochrome superfamily appears to have independently evolved beyond red/far-red photocycles in both prokaryotes and eukaryotes. Future studies on algal phytochromes should allow identification of the protein-chromophore interactions that tune their photocycles. Such information could allow engineering of plant growth responses into new spectral windows, for example, by introduction of suitably engineered phytochromes into null backgrounds (17, 18). Research on bilin-based synthetic photobiology and optogenetic applications (51) will also likely benefit from studies of algal phytochromes, because these proteins provide spectrally diverse components from eukaryotic systems.

Our studies reveal that algae ranging from tiny prasinophytes to majestic kelp forests contain functional phytochrome photoreceptors. Heterokont and prasinophyte algae contribute significantly to carbon fixation in the world's oceans (23, 52, 53), and multicellular brown algae are important for coastal ecosystems (54). It is tempting to speculate about the functions of these diverse

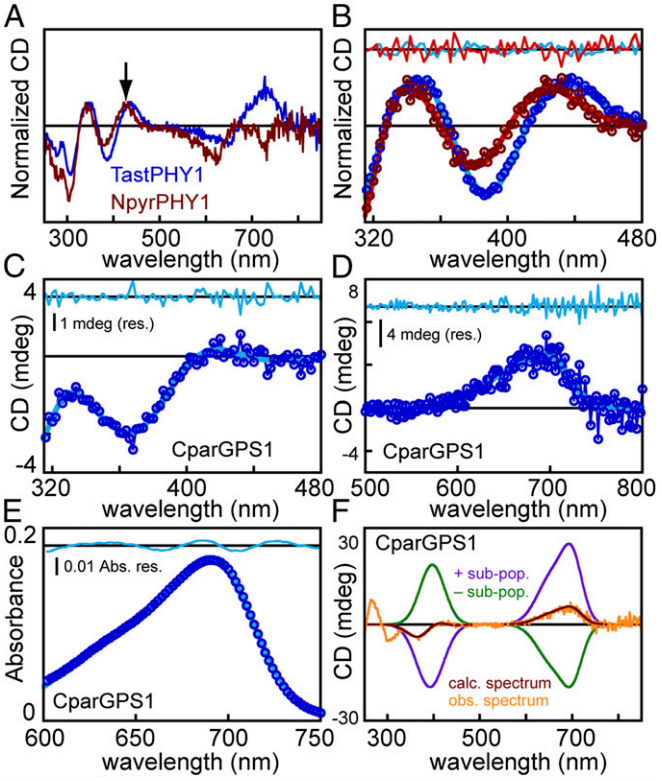

Fig. 5. Decomposition of far-red–absorbing subpopulations by CD spectroscopy. (*A*) P_{fr} CD spectra for TastPHY1 (dark blue) and NpyrPHY1 (dark red) were normalized on the indicated band (arrow). (*B*) The region from 315 to 480 nm was fit to three Gaussian functions, two of which corresponded to the bilin region of the spectrum and had similar peak wavelengths but opposing signs. Residuals are shown above (cyan and red for TastPHY1 and NpyrPHY1, respectively). (*C*) The CparGPS1 P_{fr} CD spectrum from 315 to 480 nm was analyzed as in *B*. (*D*) The CparGPS1 P_{fr} CD spectrum from 500 to 800 nm was fit to two Gaussian functions. (*E*) The P_{fr} absorption spectrum of CparGPS1 from 600 to 750 nm was fit to two Gaussian functions as in *D*. (*F*) CD spectra for two subpopulations with opposing Soret sign were constructed for CparGPS1 starting with Gaussian functions from *C*. Gaussians for the far-red region (*D*) were then scaled based on the mean relative intensities of the far-red and Soret bands for the *15Z* states of one-Cys phytochromes in this study, with one inverted (the negative P_{fr} population) and the other increased by 10% to approximate the net excess + signal in this region. The scaled far-red Gaussians were then added to the Soret Gaussians to give two complete P_{fr} spectra with opposite signs (green, purple). Their sum (dark red) is compared with the observed P_{fr} CD spectrum of CparGPS1 (orange). Parameters from fits in *B*–*E* are reported in Table S2. Experimental CD signals below 330 nm can be associated with amino acid side-chain signals and carbonyl $n\rightarrow\pi^*$ transitions (49) and were not modeled.

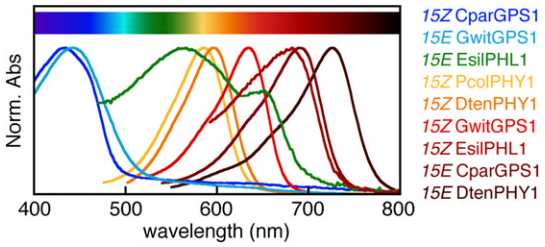

Fig. 6. Full coverage of the visible spectrum by algal phytochromes. Normalized absorption peaks are shown for the indicated algal phytochromes. Approximate color ranges within the visible region for humans are indicated on the color bar.

phytochromes. Unfortunately, a lack of research tools precludes functional analysis at the present time, and systematic studies of distribution have not been performed. We have therefore examined the available information about the habitats in which these algae have been recorded. TastPHY1 from *T. astigmatica* is the only red/far-red phytochrome reported in this study, and *T. astigmatica* was originally collected from a salt marsh (55). Ambient light conditions in such a shallow-water environment are presumably similar to conditions in shallow freshwater ponds where charophyte algae are frequently found, and charophyte phytochromes also have red/far-red photocycles (26, 28). In contrast, *Dolichomastix tenuilepis* has been recorded at the surface (0- to 2-m depth) in coastal marine environments (56, 57). *Nephroselmis pyriformis* has also been recorded in coastal marine environments, at 0- to 30-m depth (57–59), and *Prasinoderma coloniale* has been recorded from coastal and open waters from the surface to depths of 150 m (59–61). In such waters, particularly at depth, red light intensity is known to be quite attenuated (19). The blue-shifted dark states observed in NpyrPHY1, DtenPHY1, and PcolPHY1 may provide these organisms with a greater ability to detect light under such light-limited conditions.

Whereas prasinophyte phytochrome dark states can be blue-shifted relative to those of red/far-red phytochromes such as Cph1, the EsilPHL1 dark state is instead red-shifted. *E. siliculosus* resides in intertidal and sublittoral zones [0–30 m (62, 63)]. Therefore, this protein might function as a specialized sensor for detecting far-red light when the organism is at or near the surface. Multiple phytochromes are found both in *Ectocarpus* and in the related phaeophyte alga *Saccharina japonica* (64), a commercially important food source. The apparent conservation of *Ectocarpus* phytochromes in *Saccharina* (64) implies that phaeophyte phytochromes may have undergone gene family expansion. Similar expansion is seen with other signaling molecules in *Ectocarpus* (24) and with land plant phytochromes (2, 3), suggesting specialized roles for individual phytochromes in multicellular algae. Phaeophyte phytochromes may thus provide a rich field for physiological studies in the future.

Alone among the phytochromes in this study, CparGPS1 and GwitGPS1 come from freshwater organisms. Both *Cyanophora* and *Gloeochaete* have been reported in shallow freshwater environments such as ditches or seasonal ponds, typically at low densities in the presence of other algae (65, 66). This environment thus overlaps with that of charophytes, whose phytochromes have red-absorbing dark states similar to that of GwitGPS1 (26, 28). However, glaucophyte GPS proteins are distinct in that both examples studied to date have one photostate sensitive to blue light at 430–450 nm (Table S1), close to the optimal wavelength for light penetrance in a water column (19). The physiological advantage of such sensitivity for glaucophytes is currently unclear, as is the significance of the reversed red/blue and blue/far-red photocycles of GwitGPS1 and CparGPS1 relative to each other. Both *Cyanophora* and *Gloeochaete* contain multiple phytochromes (Fig. S2), but it is not clear whether this is attributable to the presence of a small family of orthologs, as in the plant phytochrome family, or attributable to the presence of spectrally and functionally diverse sensors, as in CBCRs (2, 3, 50).

The mechanistic basis for sensing blue light with bilins is well documented through studies of CBCRs: a second Cys residue forms a covalent linkage to the C10 methine bridge of the bilin chromophore, shortening the conjugated system and blue-shifting the absorption (42, 43, 67, 68). One such naturally occurring two-Cys photocycle has been reported in phytochromes to date, in the cyanobacterial protein NpF1183 (42). In NpF1183, the second Cys residue (CysD in Fig. S2) is immediately C-terminal to the Cys residue attached to the A-ring (CysC). CparGPS1 also has the CysD residue, so it is likely that its blue/far-red photocycle has a similar mechanistic basis. In contrast, GwitGPS1 lacks both CysD and the known second Cys residues found in CBCRs. It is possible that another nucleophile can form a linkage to C10 in GwitGPS1, or it is possible that a Cys residue found in GwitGPS1 and in two related *G. wittrockiana* proteins (CysB in Fig. S2) performs this role. CysB is not predicted to be near the C10 bridge based on available structural information (10–12, 69, 70), but we cannot presently rule out structural rearrangements in GPS proteins.

Finally, the CD spectra presented in this study provide evidence for chromophore heterogeneity in the P_{fr} states of algal phytochromes. Similar Soret CD signals are observed in the P_{fr} states of TastPHY1, NpyrPHY1, and CparGPS1 irrespective of the CD signs associated with the far-red band. We interpret this behavior as arising from two chromophore populations with opposed CD but similar peak wavelengths, an interpretation that allows successful modeling of the experimental spectrum of CparGPS1 (Fig. 5). Similar Soret features are seen in Cph1 and in plant phytochromes (32, 45, 46); therefore, a similar interpretation would seem likely for those proteins as well. We conclude that significant structural heterogeneity of the bilin configuration itself must exist in the P_{fr} state, even though previous studies demonstrate structural rigidity of the phytochrome P_{fr} state (71) and apparent P_{fr} homogeneity on an ultrafast timescale (72). This analysis thus alters the current view of the chromophore structure in the far-red–sensing state. These studies on algal phytochromes have extended our knowledge of phytochrome diversity and photochemistry, while also presaging future studies into algal photobiology.

Materials and Methods

Details are described in *SI Materials and Methods*. This includes information on expression and purification of algal phytochromes and on their characterization by absorption and CD spectroscopy and by acid denaturation. The fitting procedure used for Fig. 5 is also presented.

ACKNOWLEDGMENTS. We thank the Gordon and Betty Moore Foundation (GBMF) Marine Microbial Eukaryote Transcriptome Sequencing Project for sequencing and assembling algal transcriptome contigs and S. Sudek and A. Reyes-Prieto for growing these algae. This work was supported by National Institutes of Health Grant R01 GM068552 and US Department of Agriculture National Institute of Food and Agriculture Hatch Project CA-D*-MCB-4126-H (to J.C.L.), National Science Foundation Grants MGSP 0625440 and MCB 0946258 (to D.B.), and Department of Defense Grant DE-SC0004765, the Packard Foundation, and a GBMF Investigator award (to A.Z.W.).

1. Rockwell NC, Su YS, Lagarias JC (2006) Phytochrome structure and signaling mechanisms. *Annu Rev Plant Biol* 57:837–858.
2. Franklin KA, Quail PH (2010) Phytochrome functions in *Arabidopsis* development. *J Exp Bot* 61(1):11–24.
3. Mathews S (2006) Phytochrome-mediated development in land plants: Red light sensing evolves to meet the challenges of changing light environments. *Mol Ecol* 15(12):3483–3503.
4. Chen M, Chory J (2011) Phytochrome signaling mechanisms and the control of plant development. *Trends Cell Biol* 21(11):664–671.
5. Casal JJ (2013) Photoreceptor signaling networks in plant responses to shade. *Annu Rev Plant Biol* 64:403–427.
6. Hughes J (2013) Phytochrome cytoplasmic signaling. *Annu Rev Plant Biol* 64:377–402.
7. Falciatore A, Bowler C (2005) The evolution and function of blue and red light photoreceptors. *Curr Top Dev Biol* 68:317–350.
8. Rockwell NC, Lagarias JC (2010) A brief history of phytochromes. *ChemPhysChem* 11(6):1172–1180.
9. Auldridge ME, Forest KT (2011) Bacterial phytochromes: More than meets the light. *Crit Rev Biochem Mol Biol* 46(1):67–88.

10. Wagner JR, Brunzelle JS, Forest KT, Vierstra RD (2005) A light-sensing knot revealed by the structure of the chromophore-binding domain of phytochrome. *Nature* 438(7066):325–331.
11. Essen LO, Mailliet J, Hughes J (2008) The structure of a complete phytochrome sensory module in the Pr ground state. *Proc Natl Acad Sci USA* 105(38):14709–14714.
12. Yang X, Kuk J, Moffat K (2008) Crystal structure of *Pseudomonas aeruginosa* bacteriophytochrome: Photoconversion and signal transduction. *Proc Natl Acad Sci USA* 105(38):14715–14720.
13. Hughes J (2010) Phytochrome three-dimensional structures and functions. *Biochem Soc Trans* 38(2):710–716.
14. Song C, et al. (2011) Two ground state isoforms and a chromophore D-ring photoflip triggering extensive intramolecular changes in a canonical phytochrome. *Proc Natl Acad Sci USA* 108(10):3842–3847.
15. Yang X, Ren Z, Kuk J, Moffat K (2011) Temperature-scan cryocrystallography reveals reaction intermediates in bacteriophytochrome. *Nature* 479(7373):428–432.
16. Song C, et al. (2014) The D-ring, not the A-ring, rotates in *Synechococcus* OS-B′ phytochrome. *J Biol Chem* 289(5):2552–2562.
17. Strasser B, Sánchez-Lamas M, Yanovsky MJ, Casal JJ, Cerdán PD (2010) *Arabidopsis thaliana* life without phytochromes. *Proc Natl Acad Sci USA* 107(10):4776–4781.
18. Hu W, et al. (2013) Unanticipated regulatory roles for *Arabidopsis* phytochromes revealed by null mutant analysis. *Proc Natl Acad Sci USA* 110(4):1542–1547.
19. Morel A (1988) Optical modeling of the upper ocean in relation to its biogenous matter content (case I waters). *J Geophys Res* 93(C9):10749–10768.
20. Bird CJ, Greenwell M, McLachlan J (1983) Benthic marine algal flora of the north shore of Prince Edward Island (Gulf of St. Lawrence), Canada. *Aquat Bot* 16(4): 315–335.
21. Collén J, et al. (2013) Genome structure and metabolic features in the red seaweed *Chondrus crispus* shed light on evolution of the Archaeplastida. *Proc Natl Acad Sci USA* 110(13):5247–5252.
22. Duanmu D, et al. (2013) Retrograde bilin signaling enables *Chlamydomonas* greening and phototrophic survival. *Proc Natl Acad Sci USA* 110(9):3621–3626.
23. Worden AZ, et al. (2009) Green evolution and dynamic adaptations revealed by genomes of the marine picoeukaryotes *Micromonas*. *Science* 324(5924):268–272.
24. Cock JM, et al. (2010) The *Ectocarpus* genome and the independent evolution of multicellularity in brown algae. *Nature* 465(7298):617–621.
25. Price DC, et al. (2012) *Cyanophora paradoxa* genome elucidates origin of photosynthesis in algae and plants. *Science* 335(6070):843–847.
26. Kidd DG, Lagarias JC (1990) Phytochrome from the green alga *Mesotaenium caldariorum*. Purification and preliminary characterization. *J Biol Chem* 265(12):7029–7035.
27. Wu SH, McDowell MT, Lagarias JC (1997) Phycocyanobilin is the natural precursor of the phytochrome chromophore in the green alga *Mesotaenium caldariorum*. *J Biol Chem* 272(41):25700–25705.
28. Jorissen HJ, Braslavsky SE, Wagner G, Gärtner W (2002) Heterologous expression and characterization of recombinant phytochrome from the green alga *Mougeotia scalaris*. *Photochem Photobiol* 76(4):457–461.
29. Timme RE, Bachvaroff TR, Delwiche CF (2012) Broad phylogenomic sampling and the sister lineage of land plants. *PLoS ONE* 7(1):e29696.
30. Gambetta GA, Lagarias JC (2001) Genetic engineering of phytochrome biosynthesis in bacteria. *Proc Natl Acad Sci USA* 98(19):10566–10571.
31. Fischer AJ, et al. (2005) Multiple roles of a conserved GAF domain tyrosine residue in cyanobacterial and plant phytochromes. *Biochemistry* 44(46):15203–15215.
32. Rockwell NC, Shang L, Martin SS, Lagarias JC (2009) Distinct classes of red/far-red photochemistry within the phytochrome superfamily. *Proc Natl Acad Sci USA* 106(15): 6123–6127.
33. Rockwell NC, Martin SS, Gulevich AG, Lagarias JC (2012) Phycoviolobilin formation and spectral tuning in the DXCF cyanobacteriochrome subfamily. *Biochemistry* 51(7): 1449–1463.
34. Lemaux PG, Grossman AR (1985) Major light-harvesting polypeptides encoded in polycistronic transcripts in a eukaryotic alga. *EMBO J* 4(8):1911–1919.
35. Fixen KR, Baker AW, Stojkovic EA, Beatty JT, Harwood CS (2014) Apo-bacteriophytochromes modulate bacterial photosynthesis in response to low light. *Proc Natl Acad Sci USA* 111(2):E237–E244.
36. Bowler C, et al. (2008) The *Phaeodactylum* genome reveals the evolutionary history of diatom genomes. *Nature* 456(7219):239–244.
37. Burki F, Okamoto N, Pombert JF, Keeling PJ (2012) The evolutionary history of haptophytes and cryptophytes: Phylogenomic evidence for separate origins. *Proc Biol Sci* 279(1736):2246–2254.
38. Dammeyer T, Frankenberg-Dinkel N (2008) Function and distribution of bilin biosynthesis enzymes in photosynthetic organisms. *Photochem Photobiol Sci* 7(10):1121–1130.
39. Yeh K-C, Wu S-H, Murphy JT, Lagarias JC (1997) A cyanobacterial phytochrome two-component light sensory system. *Science* 277(5331):1505–1508.
40. Wagner JR, et al. (2008) Mutational analysis of *Deinococcus radiodurans* bacteriophytochrome reveals key amino acids necessary for the photochromicity and proton exchange cycle of phytochromes. *J Biol Chem* 283(18):12212–12226.
41. Berkelman TR, Lagarias JC (1986) Visualization of bilin-linked peptides and proteins in polyacrylamide gels. *Anal Biochem* 156(1):194–201.
42. Rockwell NC, Martin SS, Feoktistova K, Lagarias JC (2011) Diverse two-cysteine photocycles in phytochromes and cyanobacteriochromes. *Proc Natl Acad Sci USA* 108(29): 11854–11859.
43. Rockwell NC, et al. (2008) A second conserved GAF domain cysteine is required for the blue/green photoreversibility of cyanobacteriochrome Tlr0924 from *Thermosynechococcus elongatus*. *Biochemistry* 47(27):7304–7316.
44. Falk H (1989) *The Chemistry of Linear Oligopyrroles and Bile Pigments* (Springer, Vienna).
45. Litts JC, Kelly JM, Lagarias JC (1983) Structure-function studies on phytochrome. Preliminary characterization of highly purified phytochrome from *Avena sativa* enriched in the 124-kilodalton species. *J Biol Chem* 258(18):11025–11031.
46. Borucki B, et al. (2003) Mechanism of Cph1 phytochrome assembly from stopped-flow kinetics and circular dichroism. *Biochemistry* 42(46):13684–13697.
47. Rockwell NC, Martin SS, Lagarias JC (2012) Red/green cyanobacteriochromes: Sensors of color and power. *Biochemistry* 51(48):9667–9677.
48. Rockwell NC, Martin SS, Lagarias JC (2012) Mechanistic insight into the photosensory versatility of DXCF cyanobacteriochromes. *Biochemistry* 51(17):3576–3585.
49. Borucki B, Otto H, Meyer TE, Cusanovich MA, Heyn MP (2005) Sensitive circular dichroism marker for the chromophore environment of photoactive yellow protein: Assignment of the 307 and 318 nm bands to the n —> pi* transition of the carbonyl. *J Phys Chem B* 109(1):629–633.
50. Ikeuchi M, Ishizuka T (2008) Cyanobacteriochromes: A new superfamily of tetrapyrrole-binding photoreceptors in cyanobacteria. *Photochem Photobiol Sci* 7(10):1159–1167.
51. Tabor JJ, Levskaya A, Voigt CA (2011) Multichromatic control of gene expression in *Escherichia coli*. *J Mol Biol* 405(2):315–324.
52. Armbrust EV (2009) The life of diatoms in the world's oceans. *Nature* 459(7244): 185–192.
53. Karl DM, Church MJ, Dore JE, Letelier RM, Mahaffey C (2012) Predictable and efficient carbon sequestration in the North Pacific Ocean supported by symbiotic nitrogen fixation. *Proc Natl Acad Sci USA* 109(6):1842–1849.
54. Steneck RS, et al. (2002) Kelp forest ecosystems: Biodiversity, stability, resilience and future. *Environ Conserv* 29(4):436–459.
55. Hori T, Norris RE, Chihara M (1982) Studies on the ultrastructure and taxonomy of the genus Tetraselmis (Prasinophyceae). 1. Subgenus Tetraselmis. *Bot Mag Tokyo* 95(1037): 49–61.
56. Throndsen J, Zingone A (1997) Dolichomastix tenuilepis sp nov., a first insight into the microanatomy of the genus Dolichomastix (Mamiellales, Prasinophyceae, Chlorophyta). *Phycologia* 36(3):244–254.
57. Thomsen HA, Buck KR (1998) Nanoflagellates of the central California waters: Taxonomy, biogeography and abundance of primitive, green flagellates (Pedinophyceae, Prasinophyceae). *Deep Sea Res Part II Top Stud Oceanogr* 45(8-9):1687–1707.
58. Moestrup O (1983) Further studies on *Nephroselmis* and its allies (Prasinophyceae). The question of the genus *Bipedinomonas*. *Nord J Bot* 3(5):609–627.
59. Marin B, Melkonian M (2010) Molecular phylogeny and classification of the Mamiellophyceae class. nov. (Chlorophyta) based on sequence comparisons of the nuclear- and plastid-encoded rRNA operons. *Protist* 161(2):304–336.
60. Hasegawa T, et al. (1996) *Prasinoderma coloniale* gen. et sp nov., a new pelagic coccoid prasinophyte from the western Pacific Ocean. *Phycologia* 35(2):170–176.
61. Jouenne F, et al. (2011) Prasinoderma singularis sp. nov. (Prasinophyceae, Chlorophyta), a solitary coccoid Prasinophyte from the South-East Pacific Ocean. *Protist* 162(1):70–84.
62. Norton TA, Milburn JA (1968) Direct observations on the sublittoral marine algae of Argyll, Scotland. *Hydrobiologia* 40(1):55–68.
63. Kiirikki M, Blomster J (1996) Wind induced upwelling as a possible explanation for mass occurrences of epiphytic *Ectocarpus siliculosus* (Phaeophyta) in the northern Baltic Proper. *Mar Biol* 127(2):353–358.
64. Wang WJ, Wang FJ, Sun XT, Liu FL, Liang ZR (2013) Comparison of transcriptome under red and blue light culture of *Saccharina japonica* (Phaeophyceae). *Planta* 237(4):1123–1133.
65. Schumacher GJ, Whitford LA (1961) Additions to the fresh-water algae in North Carolina V. *J Elisha Mitchell Sci Soc* 77(2):274–280.
66. Barone R, Marrone F, Naselli-Flores L (2006) First record of Cyanophora paradoxa Korsikov (Glaucocystophyta) in Italy. *Naturalista Siciliano* S. IV, XXX(1):97–106.
67. Ishizuka T, et al. (2011) The cyanobacteriochrome, TePixJ, isomerizes its own chromophore by converting phycocyanobilin to phycoviolobilin. *Biochemistry* 50(6):953–961.
68. Burgie ES, Walker JM, Phillips GN, Jr., Vierstra RD (2013) A photo-labile thioether linkage to phycoviolobilin provides the foundation for the blue/green photocycles in DXCF-cyanobacteriochromes. *Structure* 21(1):88–97.
69. Yang X, Stojkovic EA, Kuk J, Moffat K (2007) Crystal structure of the chromophore binding domain of an unusual bacteriophytochrome, RpBphP3, reveals residues that modulate photoconversion. *Proc Natl Acad Sci USA* 104(30):12571–12576.
70. Bellini D, Papiz MZ (2012) Structure of a bacteriophytochrome and light-stimulated protomer swapping with a gene repressor. *Structure* 20(8):1436–1446.
71. Song C, et al. (2011) On the collective nature of phytochrome photoactivation. *Biochemistry* 50(51):10987–10989.
72. Kim PW, et al. (2012) Ultrafast E to Z photoisomerization dynamics of the Cph1 phytochrome. *Chem Phys Lett* 549:86–92.